JOTCS A
Journal of the Turkish Chemical Society
Section: A
Chemistry

TURKISH CHEMICAL SOCIETY

Synthesis of Manganese(II), Iron(III), and Vanadium(IV) Complexes with New Schiff Bases and their Spectroscopic and Thermal Studies and Evaluation of their Antimicrobial Activity

Sinan Al-Bayati[1], Sarab Alazawi[1*], Sadeem Al-Barody[1], Anaam Rasheed[1], Rehab Alhassani[1]

[1]Mustansiriyah University, Department of Chemistry, College of Science, Baghdad, Iraq.

Abstract: Heterocyclic 3-acetyl coumarin with hydrazide derivatives and their metal complexes are a substantial family of pharmaceutical drugs used to treat infection, anti-inflammatory issues, diabetes, and neurological disorders in the field of medicinal chemistry. Cyclization of 5- floro-2-furaldehyde, ethyl acetoacetate, and urea or thiourea by $LaCl_3.7H_2O$, addition of hydrazine to form amine derivatives were performed, and respective Schiff base derivatives (L1, L2) were produced by adding acetyl coumarin in an ethanolic solution at ambient temperature. New ligands and its complexes of the V (IV), Fe (III) and Mn (II) ions were characterized using (FT-IR, UV, MS) and nuclear magnetic resonance (1H-NMR) as well as elemental analysis (CHN). The synthesized complexes chelate with ligands L1, L2 via (N, O_2) atoms. The structural geometry of the complexes was illustrated in the solid phase using FT-IR and UV-VIS spectroscopy, elemental analysis (CHNS), and flame atomic absorption, in addition to magnetic susceptibility and conductivity measurement. The antibacterial activity of the newly prepared ligands and their metal complexes was evaluated against *Pseudonomous aerugionosa* as a gram negative and *Bacillus subtilis* as a gram positive microorganism. Moreover, the antifungal activity against two fungi *Aspergillus flavus*, and *Saccharomyces cerevisiae* was studied for all compounds. The coordinated ligands significantly increased their bactericidal and fungicidal action compared to the free ligands, which did not exhibit any activity against the selected fungal and bacterial strains. The results focused on the synergetic relationship between the metal ion and the ligand, in addition to the structural variation.

Keywords: Biological activity, metal complexes, coumarin, hydrazide derivatives, 5-fluorofuran, Schiff bases.

Submitted: February 14, 2023. **Accepted:** October 11, 2023.

Cite this: Al-Bayati S, Alazawi S, Al-Barody S, Rasheed A, Alhassani R. Synthesis of Manganese(II), Iron(III), and Vanadium(IV) Complexes with New Schiff Bases and their Spectroscopic and Thermal Studies and Evaluation of their Antimicrobial Activity. JOTCSA. 2024;11(1):101-12.

DOI: https://doi.org/10.18596/jotcsa.1250844

***Corresponding author's E-mail:** sarabmahdi@uomustansiriyah.edu.iq

1. INTRODUCTION

Flavonoids with open chain are compounds that contain an aliphatic three-carbon chain bridge with two aromatic rings that form during aldol condensation reaction (1). Chalcone is one of an important class of flavonoids; it is known as a versatile structure or an α-β-unsaturated keton that consists of active keto-ethylenic group (-CO-CH=CH) (2). Coumarins are considered a wide type of compounds in natural extracts, they are referred to as the second stage of metabolites in a number of higher-level plant species, particularly in leaves, seeds, and roots (3). Coumarin plays a vital role in controlling plant development as metabolites and have a broad range of biological activities like anti-inflammatory (4), anti-cancer, and anti-oxidant (5). Biological activity of coumarin derivetives has become an attractive target for researchers owing to its broad effects on diseases and ability to reduce harm to common cells (6).

According to previous studies, which revealed that coumarin, chalcone fibrates can down-regulate the total cholesterol (TC), phospholipids (PL) and triglycerides (TG) and regulate the levels of VLDL, LDL, and HDL, on the other side, pyrimidine serves an essential function in human proliferation as ribonucleotide

bases in RNA and as deoxyribonucleotide bases in DNA, and it has been found to contribute to multiply biological activates (7). They are considered powerful tools for treatments and possess broad, interesting biological activities such as anti-tumor and anti-fungal and they are used for thyoid drugs and leukemia (8).

Schiff bases are reported to be important ligands to coordinate with metal ion to form complexes because they are easy to prepare, have a range of structural designs, and wide range of applications. These ligands have shown remarkable performance in terms of steric properties and electronic soft tuning of their metal complexes and have been widely employed as polychelate ligands. Schiff bases are created by chemists as polydentate ligands and their complexes, and these have benefited several fields of chemistry (9).

In this work, we suggested the synthesis of new Schiff's base derivative ligands (L_1, L_2) via the reaction between hydrazide derivatives and 3-acetylcoumarin. The new ligands provide three potential donor sites for complexes with some transition metal ions. The complexes of the ligands (L1, L2) and their detailed characterization and outline of their structures are shown in (Figure 1). The prepared ligands and its complexes are candidates for potent toxic activity as antibacterial and antifungal.

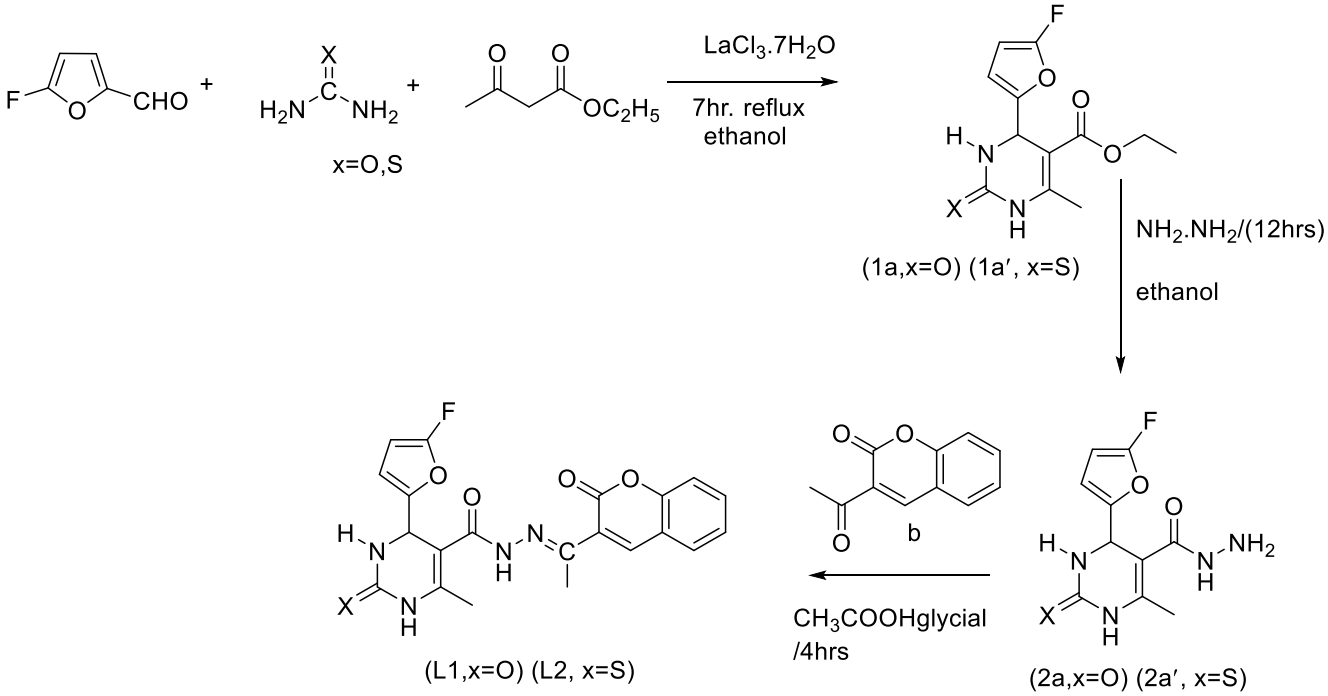

Figure 1: The route of synthesis L1, L2.

2. EXPERIMENTAL SECTION

2.1. Material and Methods

All solvents and chemicals were obtained from Sigma-Aldrich companies and used as received; there was no need for any further purification.

2.2. Instrumentation

Melting points for all synthesized compounds were recorded by a Stuart melting point (digital) SMP30 apparatus. A Shimadzu (FT-IR) model 4800s Spectrometer was used to measure the FT-IR spectrum between (4000-400) cm^{-1} using KBr discs. UV-Vis 16 ultraviolet spectrophotometer model Shimadzu is used to measure the UV -visible spectra at R.T. °C using 1-cm quartz cell and examined between 200-1100 nm at 10^{-3} M in DMSO. Atomic absorption (AA) technique has been recorded using a Shimadzu AA680G atomic absorption spectrophotometer at the laboratories of Ibn-Sinaa Company. Elemental analysis is used to determine C, H, N for the complexes of synthesized ligand [L1, L2] by Linear Regression Euro EA elemental analysis. Mass spectra was performed for ligand on GC-MS (DIRECT PROBE) via ES technique. ^{1}H, $^{13}CNMR$ spectrum for the ligands were recorded at a Bruker DMX- 5000 spectrometer (400 MHz), using DMSO-d_6 solvent. Measurement of conductivity were carried out at RT as °C in DMSO solvent for solutions of samples using an Inolab multi 740, wtw 82362-Germany. Magnetic susceptibility of novel synthesized complexes were recorded at RT °C by auto magnetic susceptibility balance in Al-Mustansiriyah University, College of science, Chemistry Department. TG and DSC (differential scanning calorimetry) thermos grams in different ranges were carried out at R.T heating rate is 10 °C/min at university Abn Al-Hathim College.

2.3. Preparation of Ligand

2.3.1. Preparation of pyrimidine derivative (1a,1á)

Ethyl-4-(5-fluorofuran-2-yl)-6-methyl-2-oxo-1,2,3,4 tetrahydropyrimidine-5-carboxylate (1a), Ethyl-4-(5-fluorofuran-2-yl)-6-methyl-2-thioxo-1,2,3,4-tetrahydropyrimidine-5-carboxylate (1á)

Ethanolic solution of urea (0.6 g, 0.01 mole) or thiourea (0.76 g, 0.01 mole) was mixed with 5-

fluoro-2-furaldehyde (1.14 g, 0.01 mole) and ethylacetoacetate (1.3 g, 0.01 mole) and lanthanum chloride heptahydrate (3.7 g, 0.01 mole) was added to this solution. The resulting mixture was poured to crushed ice (25 g) with the stirring for 10 min, the precipitate product (1a) or (1á) was filtered, and then recrystallized from ethanol after washed with cold water.

2.3.2. Preparation of hydrazide (2a, 2á)

Ethyl-4-(5-fluorofuran-2-yl)-6-methyl-2-oxo-1,2,3,4-tetrahydropyrimidine-5-carbohydrazide (2a), 4-(5-fluorofuran-2-yl)-6-methyl -2-thioxo-1,2,3,4-tetrahydropyrimidine-5-carbohydrazide (2á).

A mixture of compound (1a) (2.68 g, 0.01 mole) or compound (1á) (2.84 g, 0.01 mole) and hydrazine hydrate (2.5 g, 0.05 mole) were dissolved in 25 mL of ethanol and refluxed for 12 hours. The solid product (2a) or (2á) was collected and crystallized from ethanol.

2.3.3. Preparation of coumarin derivative (b)

The compound (b) was prepared by reacting the sailcyldehyde (1.06 g, 0.01 mole) and ethyl aceto-acetate (1.3 g, 0.01 mole) with a drop of tripropyl amine in 25 mL absolute ethanol. The product was filtered and recrystallized from ethanol (10).

2.3.4. Preparation of hydrazine Schiff base ligands (L1, L2)

Ethyl-4-(5-fluorofuran-2-yl)-6-methyl -2-oxo-N-[1-(2-oxo-2H-chromen-3-yl) ethylidene]-1,2,3,4-tetra-hydropyrimidine -5-carbohydrazide (L1).

Ethyl-4-(5-fluoro furan-2-yl)-6-methyl-N-[1-(2-oxo-2H-chromen-3-ethylidene]-2-thioxo-1,2,3,4-tetrahydro pyrimidine-5-carbohydrazide (L2).

The ligand (L1) or (L2) ware prepared by reaction compound (2a) (2.54 g, 0.01 mole) or compound (2á) (2.70 g, 0.01 mole) respectively with acetylcoumarin (b) (1.88 g, 0.01 mole) in (30 mL) absolute ethanol and drops of glacial acetic acid was added. The reaction mixture was refluxed for 4 hours, and then the product was obtained and crystallized from methanol. The physical data of synthesized ligands (L1 or L2) are described in Table 1.

2.3.5. Preparation of metal complexes

Ethanolic solution of metal ion salts, (0.228 g, 1 mmole) of $VOSO_4.5H_2O$ was added to ligand (L1) (0.424 g, 1 mmole) or (0.440 g, 1 mmole) of ligand (L2). While ethanolic solution (0.162 g, 1 mmole) of $FeCl_3.6H_2O$ or (0.198 g, 1 mmole) of $MnCl_2.4H_2O$ was added to an ethanolic solution of (2mmole of L1 or L2), respectively, and then stirred, the mixture was heated under reflux for two hours. A precipitate was formed, and the products were isolated by filtration and then recrystallized from cold ethanol. The physical properties of the prepared complexes are shown in Table 1.

Table 1: Physical properties of synthesized ligands and its complexes.

Comp.	Color	M.P. ℃	M.wt. g/mol	Elemental analysis found Calc.(%)						
				C%	H%	N%	S%	M%	M:L	Suggested formula
1a	Pale white	145-147	268.2	53.6	4.8	10.4	----	----	----	$C_{12}H_{13}FN_2O_4$
1á	Pale yellow	190-192	284.3	50.6	4.5	9.8	11.3	----	----	$C_{12}H_{13}FN_2O_3S$
2a	Brown	150-152	254.2	47.2	4.3	22.02	-----	----	----	$C_{10}H_{11}FN_4O_3$
2á	Gray	210-212	270.3	44.4	4.1	20.7	11.8	----	----	$C_{10}H_{11}FN_4O_2S$
b	Light yellow	120-122	188.2	70.1	4.3	----	----	----	----	$C_{11}H_8O_3$
L1	Yellow	115-117	424.4	93.0	6.2	20.7	----	----	----	$C_{21}H_{17}FN_4O_5$
L2	Green	218- 220	440.5	57.2	3.8	12.7	7.3	----	----	$C_{21}H_{17}FN_4O_4S$
VO-L1	Dark	123-125	580.3	43.4	3.3	9.6	---	8.7	1:1	$[VO(L1)H_2O]SO_4$
VO-L2	green	230-232	606.4	41.5	3.1	9.2	5.2	8.4	1:1	$[VO(L2)H_2O]SO_4$
Fe-L1	Brown	>300	1011.1	49.8	3.3	11.1	---	5.5	1:2	$[Fe(L1)_2]Cl_3$
Fe-L2		>300	1043.2	48.3	3.2	10.7	3.1	5.4	1:2	$[Fe(L2)_2]Cl_3$
Mn-L1	Dark	130-132	974.7	51.7	3.5	11.49	---	5.6	1:2	$[Mn(L1)_2]Cl_2$
Mn-L2	yellow	266-268	1006.8	50.0	3.3	11.1	6.3	5.4	1:2	$[Mn(L2)_2]Cl_2$

3. RESULTS AND DISCUSSION

3.1. Electronic Absorption Spectra, Magnetic Susceptibility, and Conductivity Measurements

The UV spectra of free ligand (L1) mostly showed two intense maxima of 38460 π→π* and 28493 n →π* consequently Figure 2, whereas the UV spectrum of ligand (L2) exhibited intense bands at 35080 π→π* and 29150 n→π*, respectively, Table 2.

Table 2: Electronic spectra, magnetic moment (BM) and conductance in DMF for L1, L2 and their complexes.

Compound	Maximum absorption $u_{max}(cm^{-1})$	Band Assignment	Suggested geometry	μeff. B.M	Molar Cond. $S.cm^2.mol^{-1}$
VO-L1	14084 15384 24390	$^2B_2g \rightarrow {}^2Eg_2$ $^2B_{2g} \rightarrow {}^2B_1g$ $^2B_2g \rightarrow {}^2A_1g$	Square pyramidal	2.01	86.45
VO-L2	14085 15383 24395	$^2B_2g \rightarrow {}^2Eg_2$ $^2B_{2g} \rightarrow {}^2B_1g$ $^2B_2g \rightarrow {}^2A_1g$	Square pyramidal	1.98	85.40
Fe-L1	15213 16993 33220	$^6A_2g \rightarrow {}^4T_2g$ $^6A_2g \rightarrow {}^4T_1g$ $^6A_2g \rightarrow {}^4T_1g(p)$	Octahedral	5.26	**----**
Fe-L2	15195 17022 33311	$^6A_2g \rightarrow {}^4T_2g$ $^6A_2g \rightarrow {}^4T_1g$ $^6A_2g \rightarrow {}^4T_1g(p)$	Octahedral	5.31	**----**
Mn-L1	15234 17128 34120	$^6A_2g \rightarrow {}^4T_2g$ $^6A_2g \rightarrow {}^4T_1g$ $^6A_2g \rightarrow {}^4T_1g(p)$	Octahedral	5.21	18.50
Mn-L2	15255 17328 33396	$^6A_2g \rightarrow {}^4T_2g$ $^6A_2g \rightarrow {}^4T_1g$ $^6A_2g \rightarrow {}^4T_1g(p)$	Octahedral	5.20	15.40

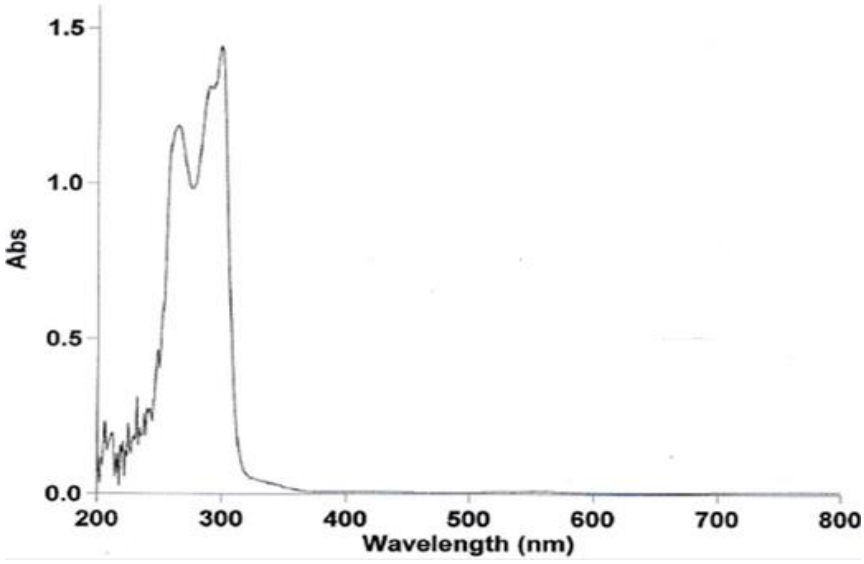

Figure 2: UV-visible spectrum of ligand L1.

3.1.1. Complexes of [V (IV)]

The product of oxovanadium VO (L1, L2) complex showed all three expected bands at [(14084, 15384, and 24390) cm^{-1} for L1 and (14084, 15384, and 24390) cm^{-1} for L2, which are assigned to $^2B_{2g} \rightarrow {}^2Eg$, $^2B_{2g} \rightarrow {}^2B1g$, and $^2B_{2g} \rightarrow {}^2A_{1g}$ transitions, respectively. These bands are characteristic to square pyramidal geometry (9, 11). The magnetic moment [(2.01 BM) for L1, (1.98 BM) for L2] is higher than the spin value of the vanadium metal only, due to a higher orbital contribution, while the conductivity measurement in DMF revealed that the complex is to be ionic (Table 2 and Figure 3).

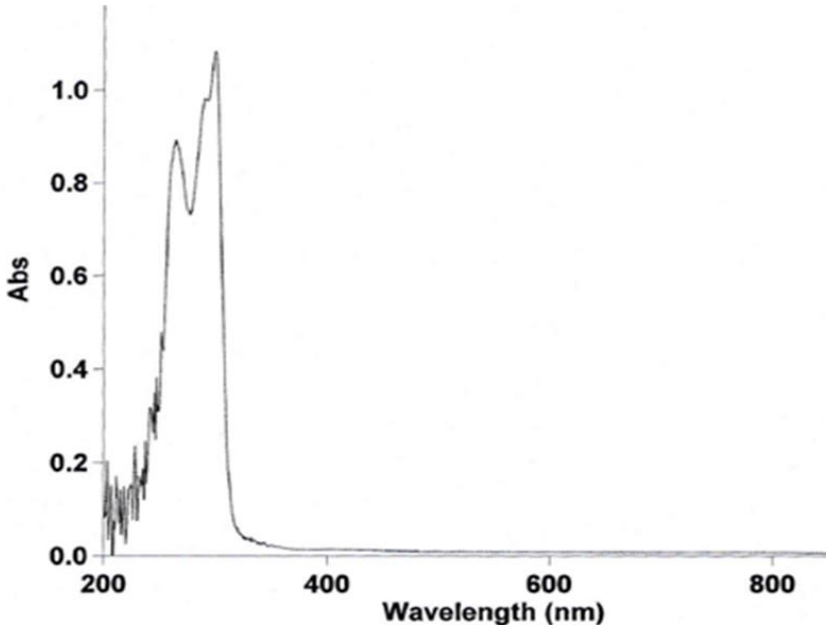

Figure 3: UV-visible spectrum of ligand VO-L1.

3.1.2. Complexes of [Fe (III)]

The prepared dark brown Fe (III) complex showed three bands at (15213, 16993, and 33220) cm^{-1} for L1 (15195, 17022, and 33311) cm^{-1} for L2 which are assigned to the transitions: $^6A_{1g}\rightarrow{}^4T_{1g}$, $^6A_{1g}\rightarrow{}^4T_{2g}$, $^6A_{1g}\rightarrow{}^4T_{1g(p)}$, and (L1, L2)→Fe (C.T), respectively, (12-14). The magnetic moment (5.26 BM), (5.31 BM) for L1, L2 respectively, with five unpaired electrons confirming an octahedral configuration (15, 16). The conductivity measurement in DMF showed that the complex was a higher conductor (Table 2); therefore, the three (Cl) atoms were not considered to be coordinated with metal ions and were located outside the coordination zone.

3.1.3. Complexes of [Mn(II)]

The UV/VIS spectrum of the Mn(II) complex displayed weak absorption bands at 15234, 17128, and 34120 cm^{-1} for L1, 15255, 17328, and 33396 cm^{-1} for L2, which were characteristic of the octahedral geometry of this complex. These bands may be assigned to $^6A_{1g}\rightarrow{}^4T_{1g}$, $^6A_{1g}\rightarrow{}^4T_{2g}$, and $^6A_{1g}\rightarrow{}^4T_{1g(p)}$ transitions, respectively (17-20). The magnetic moment (5.21 BM for L1, 5.18 BM for L2) (21), with five unpaired electrons, is in the expected range of octahedral geometry around the central metal ion (11) and showed that the complex has a high spin, conductivity measurement in DMF showed that the complex was nonionic (Table 2 and Figure 4).

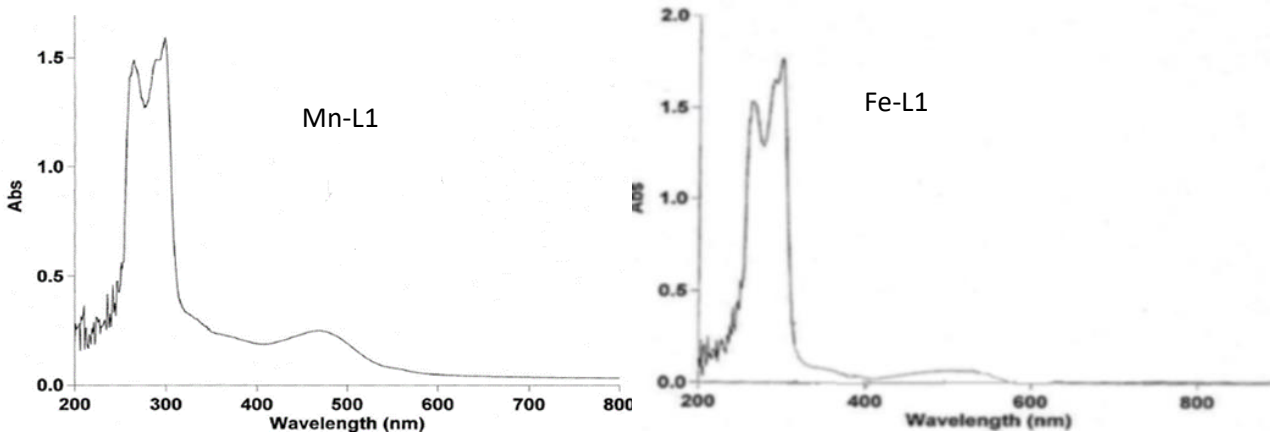

Figure 4: UV-visible spectrum of Mn-L1 and Fe-L1 Complexes.

3.2. Nuclear Magnetic Resonance Data

In the HNMR spectra of the newly synthesized ligand L1, L2, protons of NH (iminol) were observed as singlets at 9.3 ppm and 8.9 ppm as singlets were attributed to NH-pyrimidine ring, as expected. While the aromatic protons appeared at 6.4-7.92 ppm. The protons of furanyl ring were observed at 4.3-5.4 ppm and the protons of methyl were also observed as expected at 3.6 ppm (22) (Figure 5).

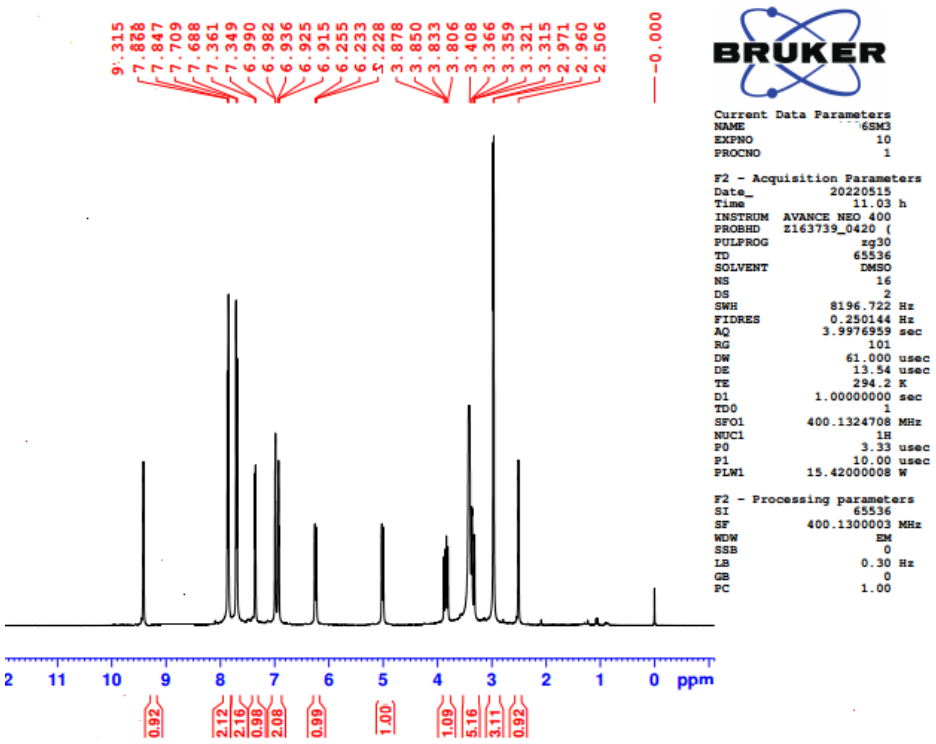

Figure 5: 1HNMR spectrum of ligands L1.

While the 1HNMR spectra for both ligand complexes showed a shift to the down field of protons of NH (iminol), which indicated a coordination with metal. Also, the carbonyl group shifted to the downfield, which confirmed coordination with the metal ion (12). The 13C-NMR spectrum of ligand (L1) is shown in Figure 6. The peaks of carbon at 118-147, 156, and 176 ppm were referred to as the aromatic carbon atoms (HC=N-) and (C=O), respectively (23) (Figure 6).

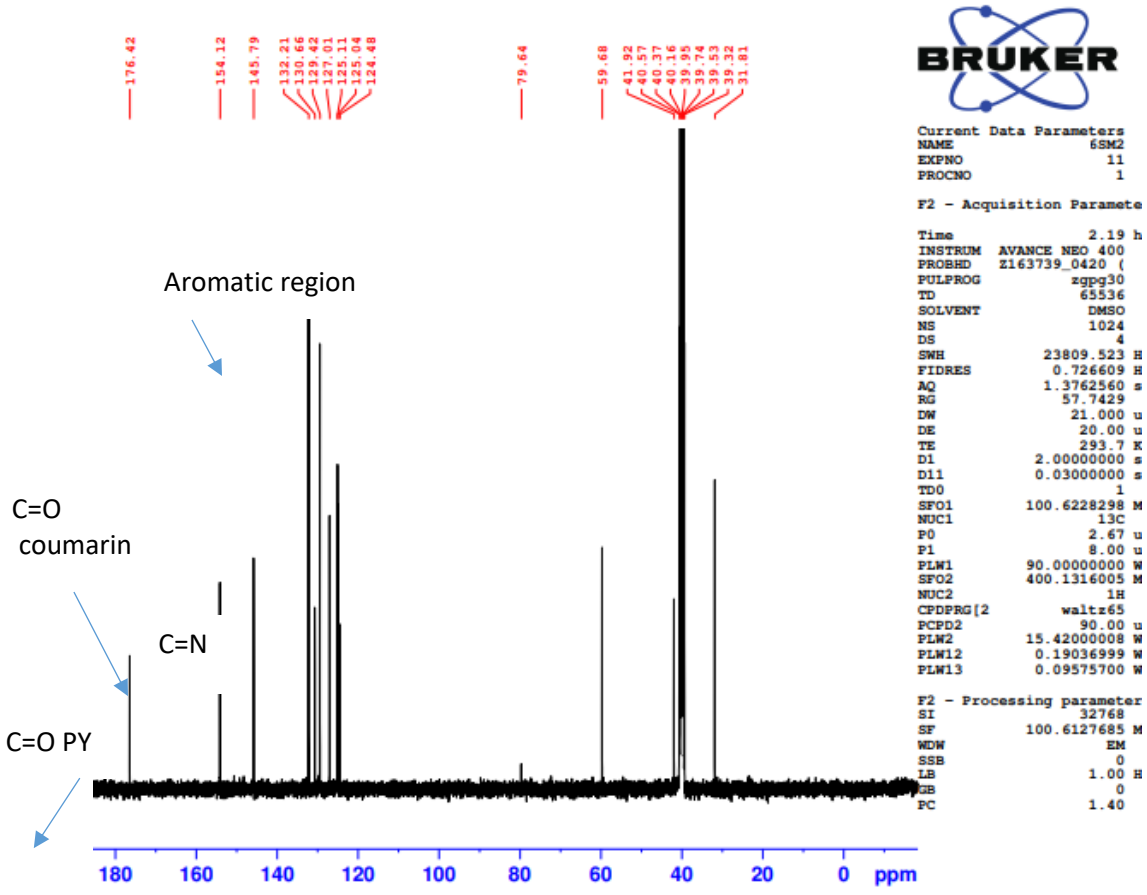

Figure 6: 13C NMR spectrum of ligands L1.

3.3. Mass Spectrum for Ligands

The positive ion mass spectral analysis of L1 is observed at m/z 425.0, which corresponds to (M+H) Figure 7. While L2 shows main peak at m/z 441, which refers to M^+.

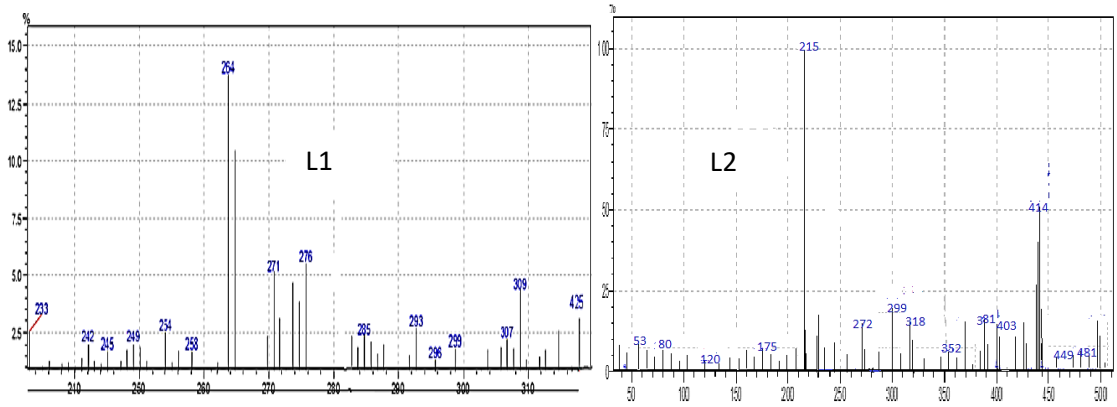

Figure 7: Mass spectra of ligands L1&L2.

3.4. FT-Infrared Spectra of Synthesized Ligands

In FTIR spectrum of ligands 1a and 1á, the amino group band (3325 cm^{-1}) and carbonyl group band (1734 cm^{-1}) of ligand **b** disappeared; instead, the newly noticeable band at 1610 cm^{-1} indicated an azomethine linkage (HC=N) (11) which proved the formation of Schiff base ligand (24). In FTIR spectra of metal complexes revealed that bands of ligand coordinated from three sites HC=N linkage, v(C=O) of coumarin ring and amide were shifted to lower frequencies (25). New weak bands were appeared in spectrum of complexes at 570-530 cm^{-1} and 460-435 cm^{-1} which assigned to v(M-N) and v(M-O) also supported the coordination (17). An intensive band at 970-960 cm^{-1} referred to V=O and confirmed the coordination of vanadium towards the ligands L1.L2 (11) (Table 3, Figure 8).

Table 3: FT-IR spectra data (cm^{-1}) for ligands and its metal complexes.

Compound formula	v(C=O) amide	v(C=N)	v(C=O) coumarin ring	M-N	M-O	M-Cl	V=O
L1	1645	1610	1715	----	----	----	----
VO-L1	960	1585	1705	570	460	390	970
Fe-L1	1630	1580	1695	565	460	380	----
Mn-L1	1640	1590	1685	560	455	390	----
L2	1650	1600	1710	----	----	----	----
VO-L2	1640	1590	1695	565	450	370	960
Fe-L2	1645	1585	1700	550	455	385	----
Mn-L2	1642	1585	1680	530	435	395	----

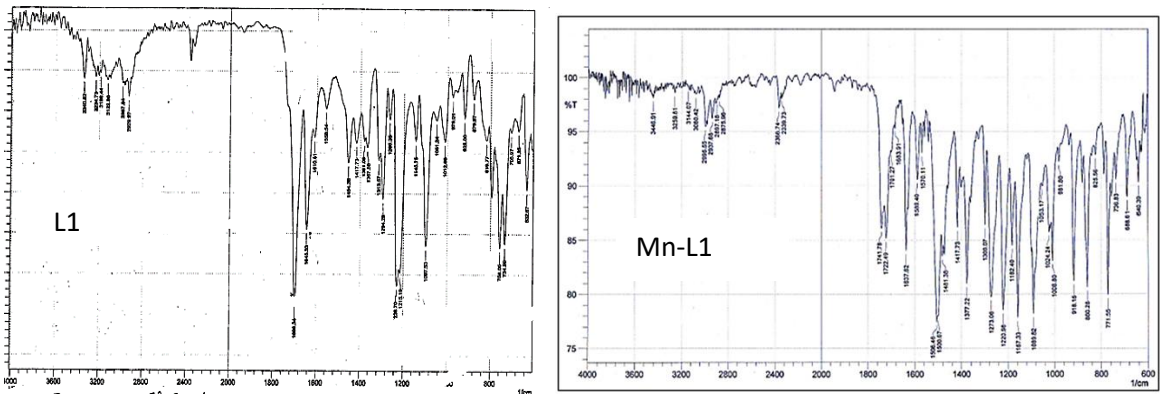

Figure 8: FT-IR spectra of ligand L1 and Mn-L1 complex.

The structure must be confirmed by FT-IR in the (4000-250) cm^{-1} region in order to show M-N.M-Cl and M-O bonds. The answer to this part (ir FT-IR) device between 4000 and 250 nm not available.

All the findings of elemental and spectral analysis, as well as magnetic moment and conductivity measurements, confirmed the suggested structure of the new compounds, as shown in the following Figure 9.

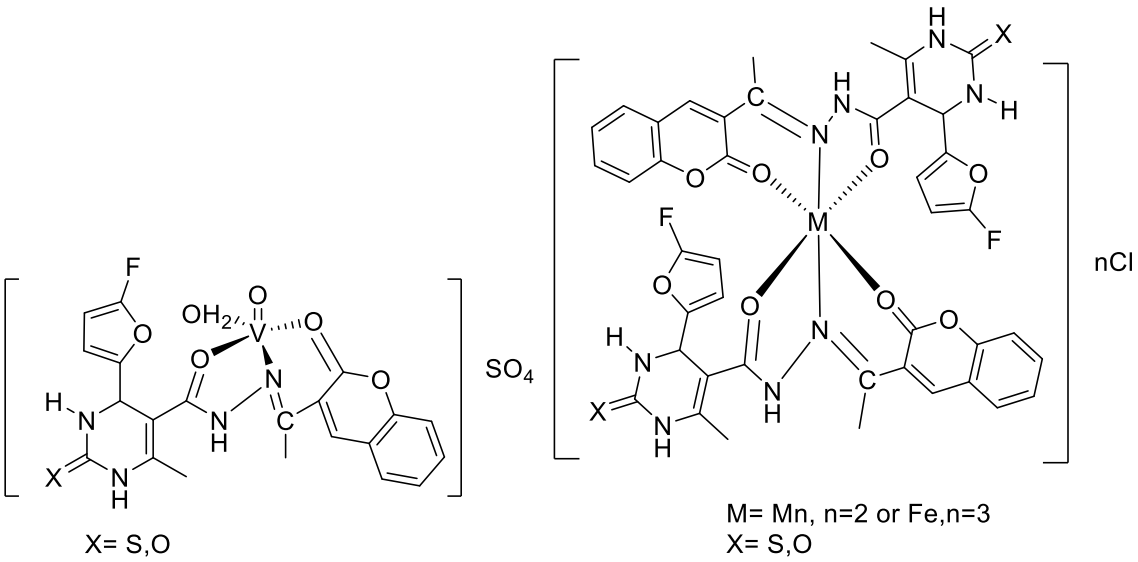

Figure 9: Proposal structure of complexes.

3.5. Thermal degradation of ligands and their complexes

Thermograms have been carried out in the range of 25 – 600 °C at a heating rate of 10 °C / min in an argon atmosphere. The results of TG suggested a mechanism for degradation $[Mn(L1)_2]Cl_2$ and $[Fe(L1)_2]Cl_3$ complexes to 351 °C. While the [L1] and [VO (L1) H_2O]Cl_2 complex was heated to 600 °C (Figure 14). The thermal degradation of [L1] is shown in Figure 10. The thermogram curve shows three decomposition steps. The TGA peak observed at 259.59 °C was assigned to the loss of (C-O) of furyl group fragment, (detd. 1.43 mg, 63%; calcd.=1.40 mg). The second step is carried out at 437.5 °C, which revealed to loss of (COO) of coumarin ring (obsd. 2.31 mg, 11.20%; calcd. =2.34 mg). A peak at 592.9 °C was observed in third step of decomposition related to the loss of CH=CHO attached to the furan ring (obsd. 2.46mg, 11.74%; calcd.= 2.30 mg). The differences in the weight may be related to a sublimation process which occurred at high temperature. The DSC curve recorded two peaks at 84.3 and 269.6 which refer to an exothermic decomposition process (18) (Figure 10). The thermal analysis clearly indicated that the complexes of $[Fe(L1)]Cl_3$ are decomposed, as shown in Figure 13. It also confirmed that the complex is stable up to 134 °C. The TGA peak is observed at 134 °C and is attributed to the loss of Cl coordination in the outer sphere (counter ions), (detd = 0.51 mg, 5.56%; calcd.= 0.5749 mg, see Figures 10, 11. TG thermogram of an argon atmosphere of $[Mn(L1)_2]Cl_2$, $[Fe(L1)_2]Cl_2$, respectively (17, 25) (Figure 13).

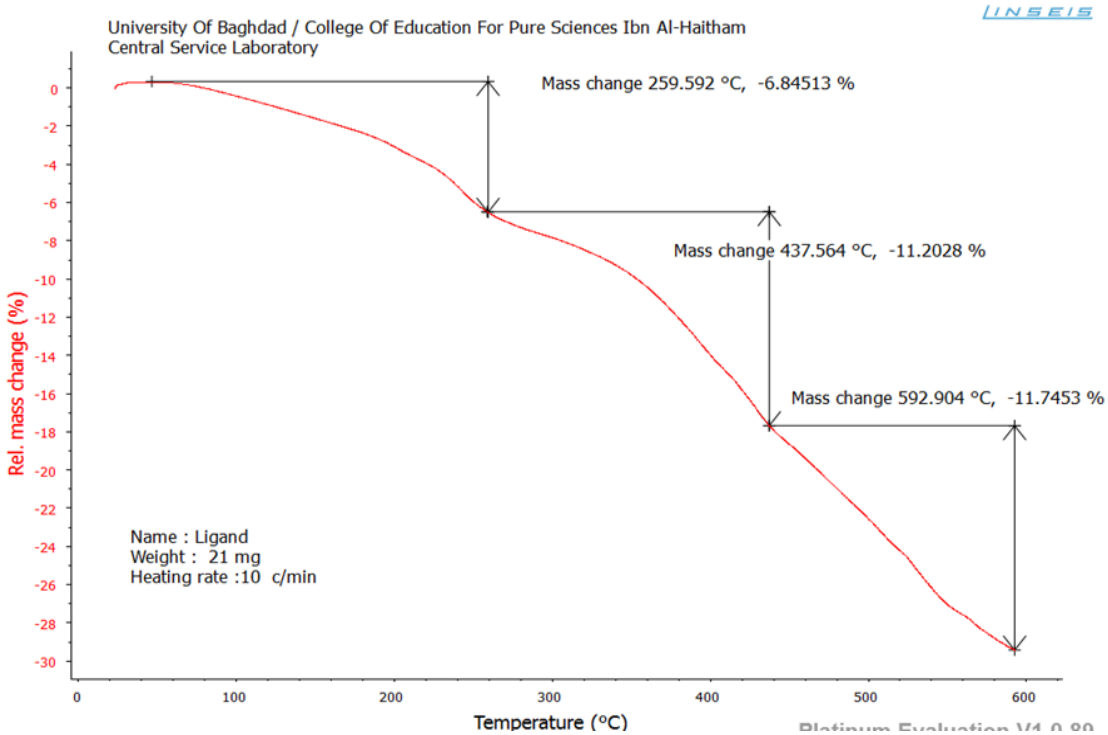

Figure 10: TG thermogram of an argon atmosphere [L1].

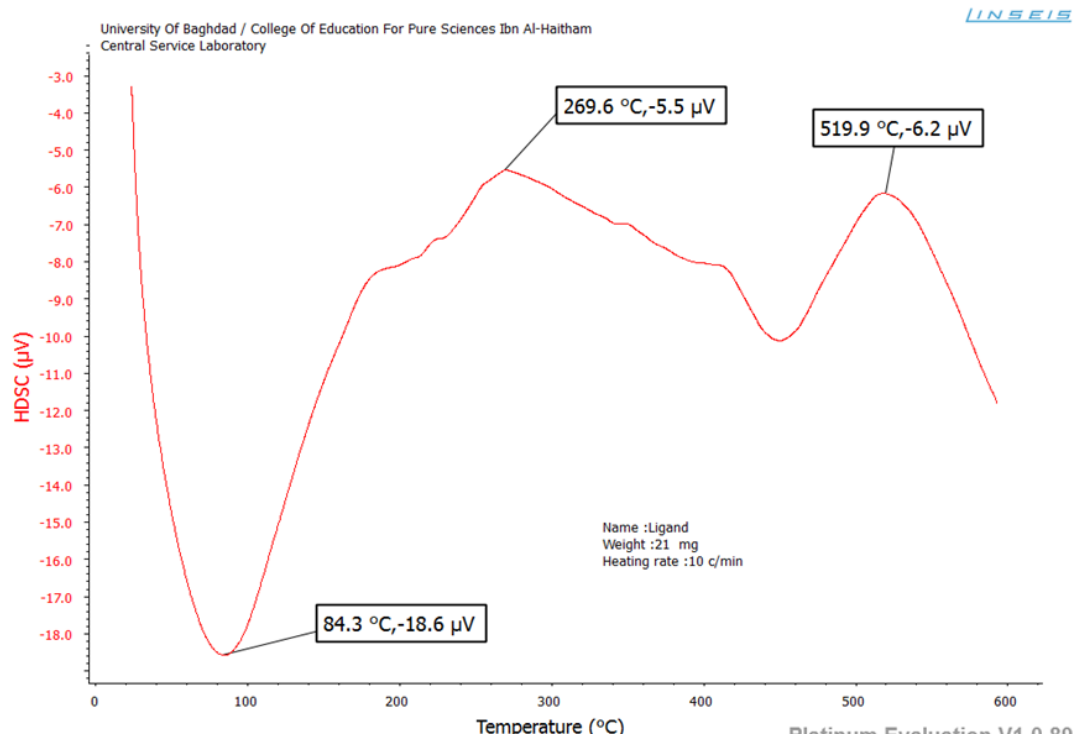

Figure 11: DSC thermogram of an argon atmosphere [L1].

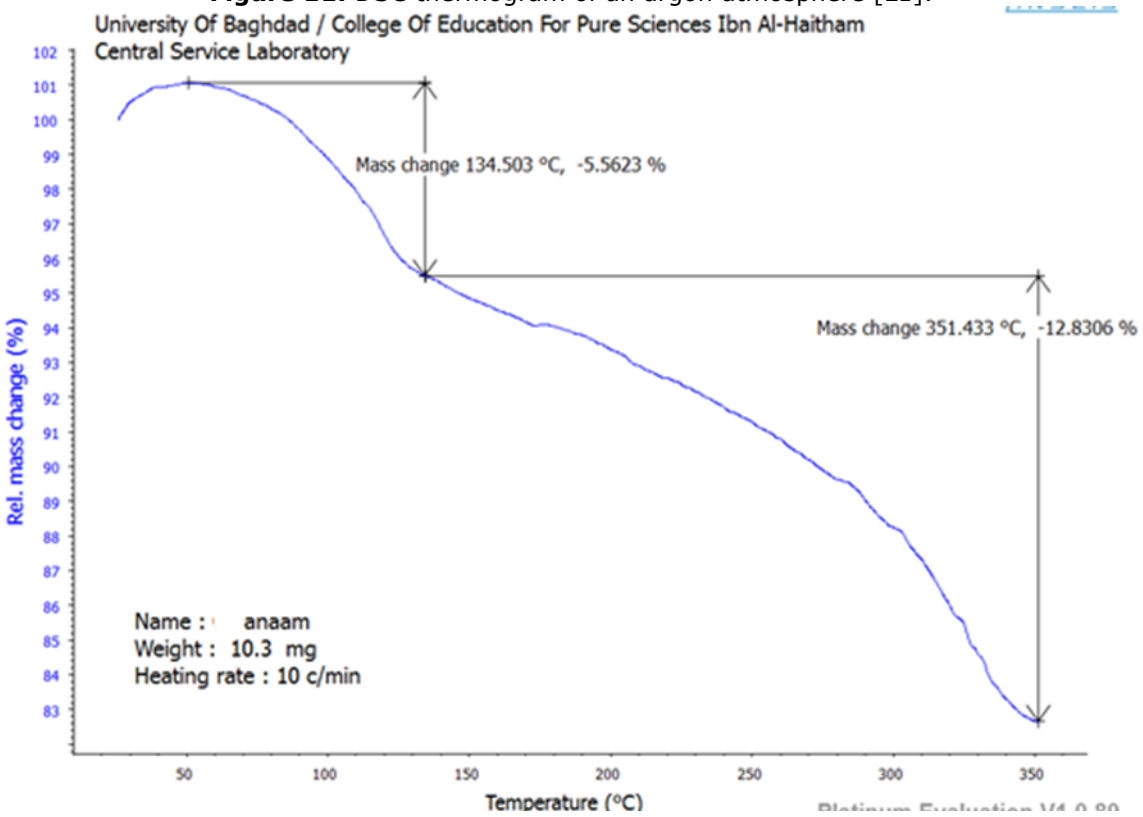

Figure 12: TG thermogram of an argon atmosphere [Mn (L1)]Cl_2.

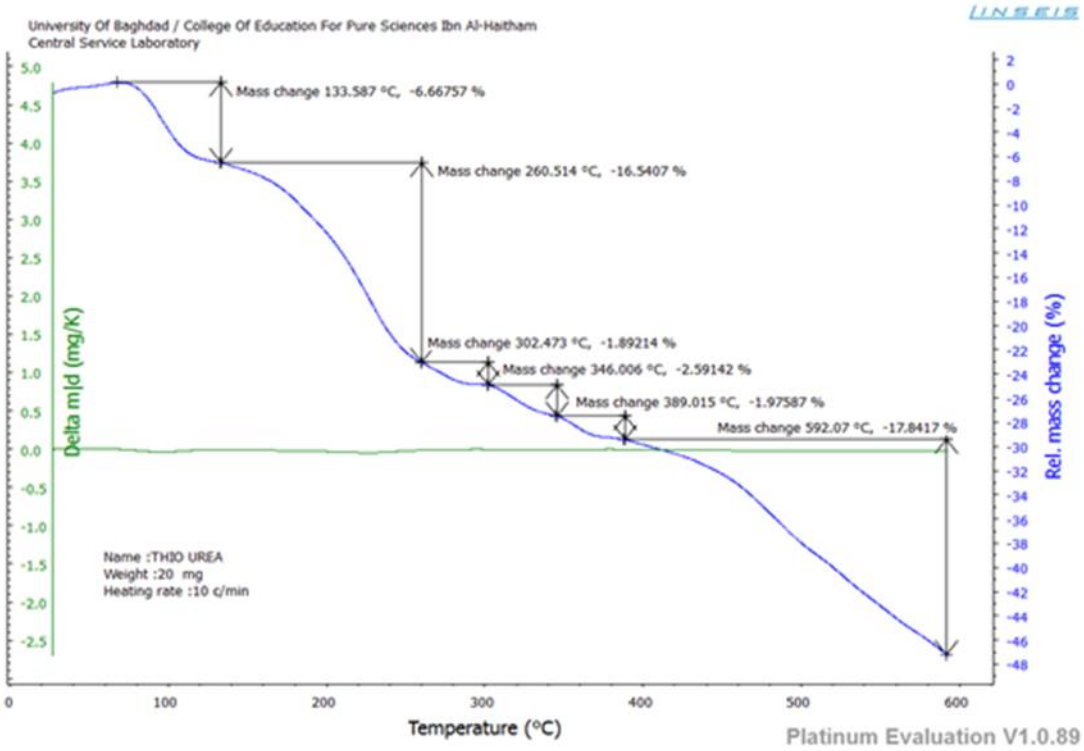

Figure 13: TG thermogram of an argon atmosphere $[Fe(L1)_2]Cl_3$.

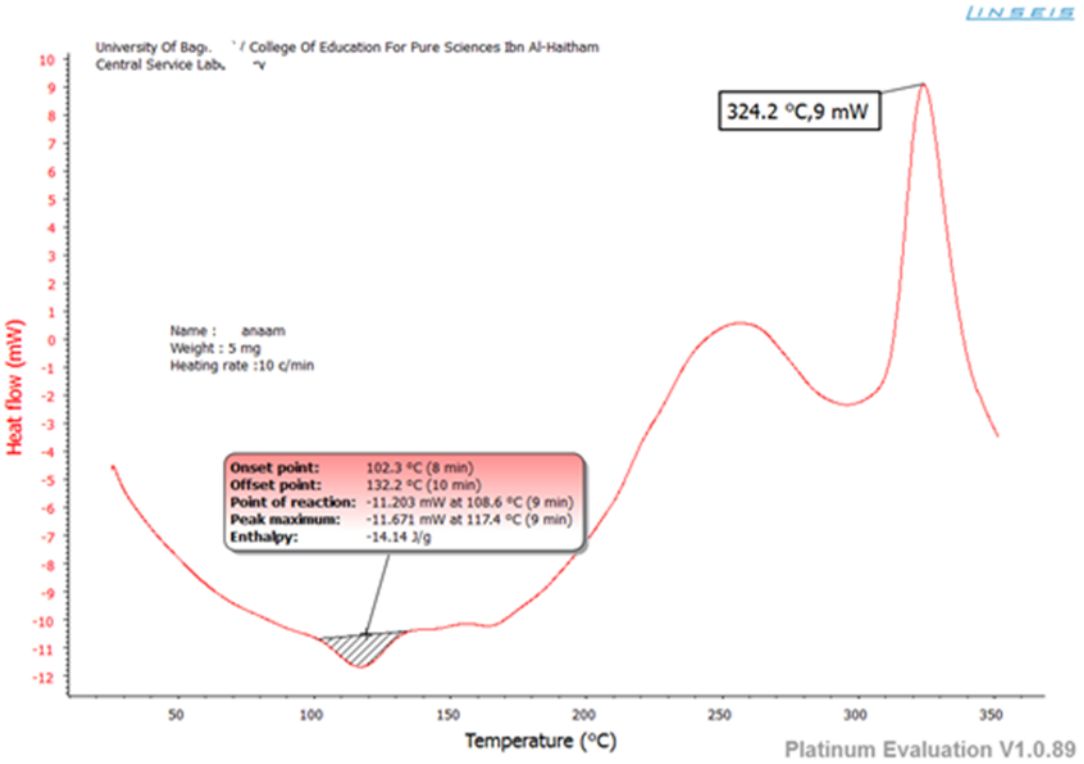

Figure 14: DSC thermogram of $[VO\ (L1)\ H_2O]Cl_2$ in argon atmosphere.

3.6. Study of Biological Activities for Ligands (L1, L2) and its Metal Antimicrobial Study

The ligands L1 and L2 and their complexes were tested *in vitro* for its capability to inhibit the growth of typical microorganisms *Pseudonomonas aerugionosa* and *Bacillus subtilis* (26). Also, it was tested against *Aspergillus flavus* and *Saccharomyces cerevisiae* fungi in DMSO as a blank solvent, (see Table 4). According to the data obtained, it can be summarized as the following:

1) L1 has high activity against both kinds of bacteria compared with activity of L2.
2) All corresponding complexes of L1 and L2 exhibited higher activity against both kinds of bacteria than the free ligands' activity (see Table 4).
3) The activity of the antifungal findings for all complexes revealed that the complexes of L1 were more toxic than complexes bearing L2, as

well as that the metal ion chelates of L1 and L2 ligands were highly toxic compared to their free ligands L1 and L2 against the same microorganisms and under the same investigational conditions (18, 27).

Table 4: Antimicrobial activities of new ligands L1 and L2 and its metal complexes.

Compound	*Pseudonomous aerugionosa*	*Bacillus subtilis*	*Saccharomyces cerevisiae*	*Aspergillus flavus*
Control DMSO	-	-	-	-
(L1)	4	4	30	38
(L2)	-	-	43	40
VOL1	6	12	25	31
VOL2	4	6	32	39
FeL1	8	10	28	33
FeL2	4	8	38	42
MnL1	8	6	29	33
MnL2	6	4	32	40
	Where: **6-8 (+)** **8-10 (++)** **>10 (+++)**		**Where:** **30-40 (+++)** **20-30 (++++)** **10-20 (++++)**	

4. CONCLUSION

In conclusion, new complexes were synthesized and characterized by spectroscopic and analytical methods. The results showed that both new synthesized ligands coordinated with ion metals via three chelating atoms (NOO). Also, it was demonstrated that V(IV) complexes have a square pyramidal structure with a ratio of (1:1, M:L), while other complexes showed a octahedral configuration around Fe(III) and Mn(II) with a ratio of (1:2, M:L). Biological results confirmed that all ligands and their corresponding complexes were tested against some bacteria and fungi and exhibited low toxic activity by ligands L1 and L2, while their corresponding complexes with L1 exhibited highly toxic activity compared to their complexes with L2, so these complexes can be candidates to be antiviral or antibacterial agents.

5. CONFLICT OF INTEREST

The authors declare no conflicts of interest.

6. ACKNOWLEDGMENTS

Great thanks from the authors to the Department of Chemistry, College of Science, Mustansiriyah University, for providing facilities and laboratories.

7. REFERENCES

1. Ahmad F, Idris MHS, Adib AM. Synthesis and characterization some flavonoids derivatives [Internet]. Research Vote: 75148. Malaysia; 2006 [cited 2023 Nov 6]. Available from: <URL>.

2. Alajrawy OI. Synthesis and characterization of vanadium (IV) and (V) complexes with 2, 2`-bipyridine ligand. 2019;

3. Patil SA, Kandathil V, Sobha A, Somappa SB, Feldman MR, Bugarin A, et al. Comprehensive Review on Medicinal Applications of Coumarin-Derived Imine–Metal Complexes. Molecules [Internet]. 2022 Aug 16;27(16):5220. Available from: <URL>.

4. Hamid SJ, Salih T. Design, Synthesis, and Anti-Inflammatory Activity of Some Coumarin Schiff Base Derivatives: In silico and in vitro Study. Drug Des Devel Ther [Internet]. 2022 Jul;16:2275–88. Available from: <URL>.

5. Melagraki G, Afantitis A, Igglessi-Markopoulou O, Detsi A, Koufaki M, Kontogiorgis C, et al. Synthesis and evaluation of the antioxidant and anti-inflammatory activity of novel coumarin-3-aminoamides and their alpha-lipoic acid adducts. Eur J Med Chem [Internet]. 2009 Jul 1;44(7):3020–6. Available from: <URL>.

6. Sahoo S, Himanshu D, Sahoo B, Sahoo SS, Shukla S, Nandy S, et al. Synthesis of novel coumarin derivatives and its biological evaluations. Eur J Exp Biol [Internet]. 2012;2(4):899–908. Available from: <URL>.

7. Bader AT, Al-qasii NAR, Shntaif AH, El Marouani M, AL Majidi MIH, Trif L, et al. Synthesis, Structural Analysis and Thermal Behavior of New 1,2,4-Triazole Derivative and Its Transition Metal Complexes. Indones J Chem [Internet]. 2022 Dec 28;22(1):223–32. Available from: <URL>.

8. Shaban S, baghi hamza, Shafek S, zein nabila, Aiad I, Omran M. Synthesis and characterization of new 1,2,4-triazole anticancer scaffold derivatives: In Vitro study. Egypt J Chem [Internet]. 2021 Mar 31;64(8):4005–15. Available from: <URL>.

9. Ndahi NP, Garba H, Waziri I, Osunlaja AA, Putaya HAN. Complexes of Mn(II) and Fe (III) with Schiff bases Derived from Trimethoprim with Salicyldehyde and Benzaldehyde as Potential Antimicrobial Agents. Niger J Pharm Biomed Res [Internet]. 2018;3(1):53–9. Available from: <URL>.

10. Al-Warhi T, Sabt A, Elkaeed EB, Eldehna WM. Recent advancements of coumarin-based anticancer agents: An up-to-date review. Bioorg Chem [Internet]. 2020 Oct 1;103:104163. Available from: <URL>.

11. Sumrra SH, Ramzan S, Mustafa G, Ibrahim M, Mughal EU, Nadeem MA, et al. Complexes of Imino-1,2,4-triazole Derivative with Transition Metals: Synthesis and Antibacterial Study. Russ J Gen Chem [Internet]. 2018 Aug 16;88(8):1707–11. Available from: <URL>.

12. Bagihalli GB, Avaji PG, Patil SA, Badami PS. Synthesis, spectral characterization, in vitro antibacterial, antifungal and cytotoxic activities of Co(II), Ni(II) and Cu(II)

complexes with 1,2,4-triazole Schiff bases. Eur J Med Chem [Internet]. 2008 Dec 1;43(12):2639–49. Available from: <URL>.

13. Singh MS, Chowdhury S, Koley S. Advances of azide-alkyne cycloaddition-click chemistry over the recent decade. Tetrahedron. 2016 Sep;72(35):5257–83.

14. Ismail AH, Al-Bairmani HK, Abbas ZS, Rheima AM. Synthesis, Characterization, Spectroscopic and Biological Studies of Zn(II), Mn(II) and Fe(II) Theophylline Complexes in Nanoscale. Nano Biomed Eng [Internet]. 2020 Sep 18;12(3):253–61. Available from: <URL>.

15. Knittl ET, Abou-Hussein AA, Linert W. Syntheses, characterization, and biological activity of novel mono- and binuclear transition metal complexes with a hydrazone Schiff base derived from a coumarin derivative and oxalyldihydrazine. Monatshefte für Chemie - Chem Mon [Internet]. 2018 Feb 27;149(2):431–43. Available from: <URL>.

16. Shukla SN, Gaur P, Raidas ML, Chaurasia B, Bagri SS. Novel NNO pincer type Schiff base ligand and its complexes of Fe(III), Co(II) and Ni(II): Synthesis, spectroscopic characterization, DFT, antibacterial and anticorrosion study. J Mol Struct [Internet]. 2021 Sep 15;1240:130582. Available from: <URL>.

17. Patil SA, Prabhakara CT, Halasangi BM, Toragalmath SS, Badami PS. DNA cleavage, antibacterial, antifungal and anthelmintic studies of Co(II), Ni(II) and Cu(II) complexes of coumarin Schiff bases: Synthesis and spectral approach. Spectrochim Acta Part A Mol Biomol Spectrosc [Internet]. 2015 Feb 25;137:641–51. Available from: <URL>.

18. Al-Zaidi BH, Hasson MM, Ismail AH. New complexes of chelating Schiff base: Synthesis, spectral investigation, antimicrobial, and thermal behavior studies. J Appl Pharm Sci [Internet]. 2019 Apr;9(4):45–57. Available from: <URL>.

19. Priya B, Kumar A, Sharma N. Synthesis, Characterisation, and Biological Properties of Oxidovanadium(IV) 3,5-Dinitrosalicylhydroxamate Complexes. Aust J Chem [Internet]. 2020;73(1):61–72. Available from: <URL>.

20. Al-Hasani RAM, Rasheed AM, AL-bayati SM. Synthesis, Characterization and Bioactivities of V(III), Cr(III), Fe(III), Rh(III) and Al(III) Complexes with Bis(Salicylaldehyde)MalonylDihydrazone and 8-HydroxyQuinoline as Mixed Ligands. Iraqi Natl J Chem [Internet]. 2016;16(3):127–42. Available from: <URL>.

21. Akkasali R, Patil N, Angadi SD. Synthesis, Characterization and Microbial Activities of Metal Complexes with Coumarine Derivatives. Rasayan J Chem [Internet]. 2009;2(1):81–6. Available from: <URL>.

22. Yaul SR, Yaul AR, Pethe GB, Aswar AS. Synthesis and characterization of transition metal complexes with N, O-chelating hydrazone Schiff base ligand. Am J Sci Res [Internet]. 2009;4(4):229–34. Available from: <URL>.

23. Martínez RF, Ávalos M, Babiano R, Cintas P, Light ME, Jiménez JL, et al. Hydrazones from hydroxy naphthaldehydes and N-aminoheterocycles: structure and stereodynamics. Tetrahedron [Internet]. 2011 Mar 18;67(11):2025–34. Available from: <URL>.

24. Golcu A, Tumer M, Demirelli H, Wheatley RA. Cd(II) and Cu(II) complexes of polydentate Schiff base ligands: synthesis, characterization, properties and biological activity. Inorganica Chim Acta [Internet]. 2005 Mar 30;358(6):1785–97. Available from: <URL>.

25. Puckett CA, Ernst RJ, Barton JK. Exploring the cellular accumulation of metal complexes. Dalt Trans [Internet]. 2010 Jan 19;39(5):1159–70. Available from: <URL>.

26. Alazawi SM, Rasheed AM, Al-Bay SM, Abed AH. Synthesis, Spectral and Biological Studies of New 2-amino-3-cyanopyridine Derivatives and Their Transition Metals Complexes. Egypt J Chem [Internet]. 2021 Mar 15;64(6):2937–44. Available from: <URL>.

27. Al-Bayati S, Rasheed A, Zuhair E, Abid K, Khamis W. Synthesis and Spectroscopic Studies of New Alkoxy Schiff Base Complexes Based on Coumarin Moiety. Am J Chem [Internet]. 2018;8(1):1–7. Available from: <URL>.